Proceedings of 12th IOE Graduate Conference
Peer Reviewed
ISSN: 2350-8914 (Online), 2350-8906 (Print)
Year: 2022 Month: October Volume: 12

Rock Excavation and Support for an Underground Powerhouse Cavern at Super Dordi Kha Hydropower Project, Nepal

Shuvam Adhikari [a], Chhatra Bahadur Basnet [b], Ghan Bahadur Shrestha [c]

[a, b, c] *Pashchimanchal Campus, IOE, Tribhuvan University, Nepal*

[a] shuvamadh@gmail.com, [b] chhatra.basnet@gmail.com, [c] gb.shrestha20@gmail.com

Abstract

Super Dordi Kha Hydropower Project is located in Lamjung, Nepal. It is located in a foliated banded gneiss rockmass. Many underground structures have been implemented in the project such as tunnels, desander caverns and pressure shafts and surge shafts. However, this paper is limited to discussing the rock excavation and support of the powerhouse cavern only. Rock engineering assessment of the study area was carried out through extensive fieldwork. The input parameters were established based on the constructed geological model, various laboratory tests, empirical formulas and stress analysis by construction of valley model. Numerical model of the underground cavern was established based on the rock excavation sequence and support used in the site.

Keywords

Himalyan Geology, Numerical model, Powerhouse cavern, Underground Structures

1. Introduction

Super Dordi Kha Hydropower Project(SDHPP) is located at Dordi Gaun Palika wards no 6 and 7, Gandaki Province, Lamjung District in Nepal as shown in Figure 4. The project is under construction and is being developed by Peoples Hydropower Company Ltd. Super Dordi Hydropower Project is a run-of-river (ROR) type of hydropower project with an installed capacity of 54MW. All the project

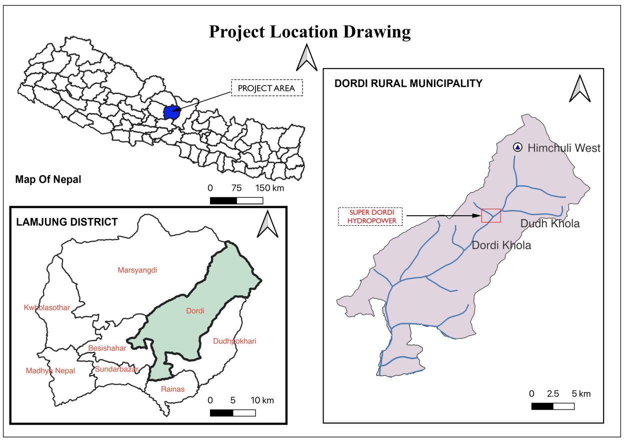

Figure 1: Project location of Super Dordi Hydropower project

structures are underground except the diversion weir and switchyard. The project comprises of 18.5 m long weir, 33.44 m long gravel trap, headrace tunnel of 4.667 km, an RCC surge tank of 49 m height and 6m diameter, 1052 m long penstock, and an underground powerhouse 38.8m long 14m wide and 28m high. The

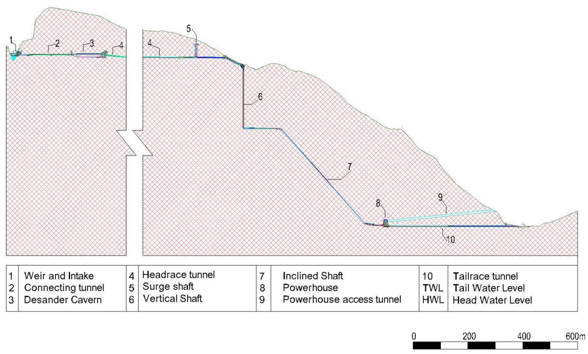

Figure 2: Project components of SDHPP

topography often dictates the layout of the facilities in hydropower projects. The main waterway including desander cavern and head race tunnels and pressure tunnels are built underground due to the long term stability provided by these structures compared to their surface conveyance options with respect to the the area's high tectonic activity and risk of landslides. Initially a surface powerhouse was proposed in the project. However, there were some structural changes in project site due to 25th April 2015 earthquake and its consequence aftershocks which caused maximum damages in the running projects in Nepal. Since , the proposed powerhouse location was in confluence of two rivers and there was also risk of landslide in uphill side. A simple letterbox shaped underground powerhouse cavern with an arched roof and vertical walls is adopted in the project. As the component housed in the powerhouse is of enormous cost and importance in hydropower projects, it is necessary to reduce any potential risk while integrating it with realistic and affordable engineering solutions [1]. The relative settlement of the arch crown, the area of the plastic zone, the area of the tensile rupture zone and the convergence of cavern walls can be chosen as the standard to assess the stability state of underground caverns.

2. Project Geology

The Super Dordi Hydropower project lies in the Higher Himalayan zone located about 10 km north of Main Central Thrust which can be identified as the Himalayan Gneisses Zone. Most of the downstream of the tunnel and powerhouse are made up of slightly–moderately worn, medium foliated, strong gneiss rock. Structurally the foliation of the gneiss mass shows gentle dipping about 0 to maximum 30 degrees towards 040 to 060 degrees (NNE) north-east upstream.

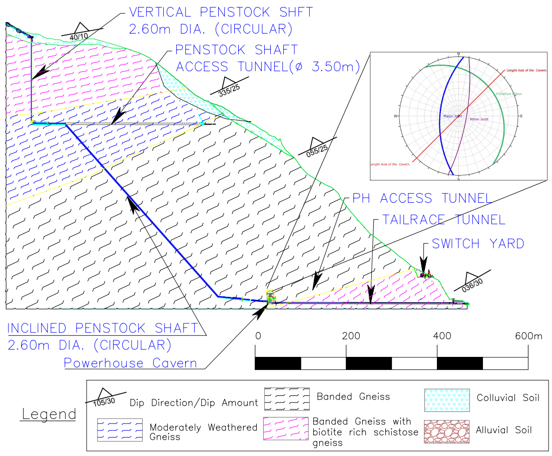

Figure 4: Engineering geological profile of the powerhouse area.

Two major joint sets with a dip amount of about 50 ° and trending W and NE were observed in the area. The majority of joint planes were fresh and tight to slightly altered. The joint surfaces were rough or irregular and smooth. The excavated rock mass was dark grey-coloured kyanite-garnet bearing banded gneiss along with biotite-rich schistose gneiss. The rock mass was in dry condition. Moderate slabbing could be observed at the crown during excavation. Quartz veins were prominent in the rock mass. The geological map of powerhouse cavern is included in the figure 3

3. Establishment of Input Parameters

3.1 Intact rock properties

Four rock core samples from SDHPP were tested in the laboratory at NTNU. The laboratory test data obtained from the laboratory is given in the Table1. The average value of different parameters obtained from the laboratory test results was used to estimate different rock mass properties.

Table 1: Laboratory test data of rocks at SDHPP

Sample	σ_{ci}(MPa)	E_m(Gpa)	ν	δ(g/cm^3)
Sd2	40.5	18.96	0.45	2.7
Sd3	43.6	24.35	0.31	2.7
Sd5	42.5	21.14	0.24	2.7
Mean	**42.2**	**21.48**	**0.33**	**2.7**
σ	**1.57**	**2.71**	**0.11**	**0**

3.2 Estimation of rock mass properties

Mechanical properties of rock mass are related to its strength and deformability properties and these properties are of utmost importance when it comes to the modelling of caverns. Apart from it, the stress conditions, presence of any weakness and shear zone and 3D topography in the project area are crucial for modelling of the caverns [2].

Compressive strength The value of rock mass strength(σ_{cm}) was calculated using the empirical formula proposed by [3] which is suitable for brittle rock mass in the Himalayas.

$$\sigma_{cm} = \frac{{\sigma_{ci}}^{1.6}}{60} \tag{1}$$

From the above equation the rock mass strength was calculated to be σ_{cm} = 6.64 MPa.

Elastic parameters The value of rock mass deformation modulus(E_{cm}) was calculated using the

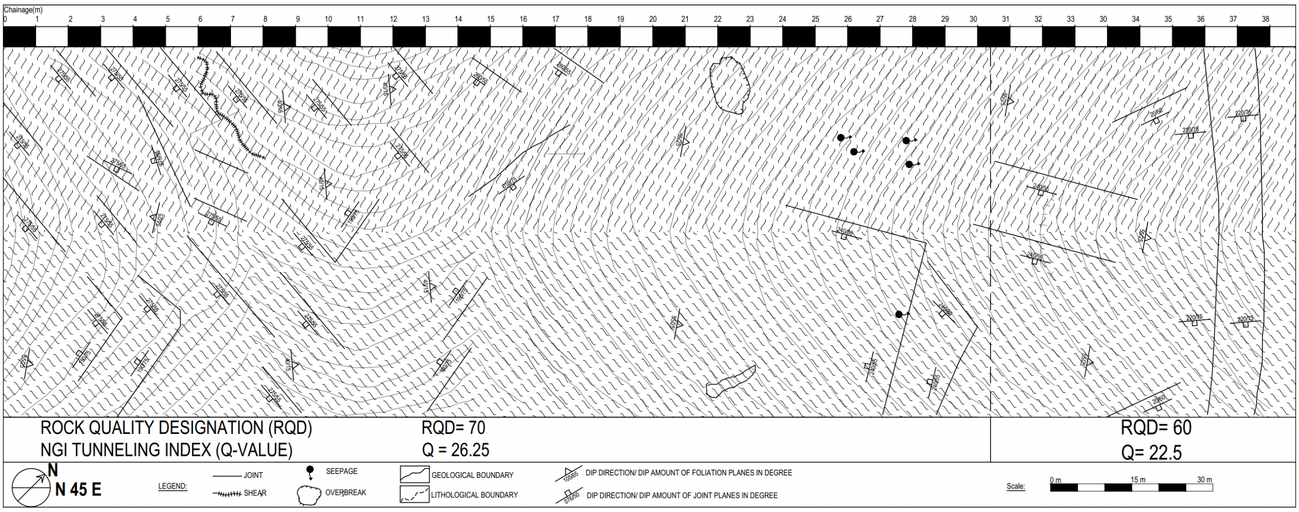

Figure 3: Geological map of the powerhouse cavern(central drift, first heading)

empirical formula proposed by [4] which is suitable for numerical modelling. The disturbance factor was taken as D = 0.3 based on the chart by [1] in the disturbed zone near the excavation boundary. The radius of the disturbed zone due to blast damage is considered to be 2m.

$$E_m = E_{ci}\left(0.02 + \frac{1-\frac{D}{2}}{1+exp(\frac{60+15D-GSI}{11})}\right) \quad (2)$$

Using above equation, the modulus of deformation was found to be $E_{cm}(undisturbed)$ = 13569.33 MPa and $E_{cm}(disturbed)$ = 7573.18 MPa..

Rock Mass Quality and GSI Joint mapping and rock mass classification were carried out in the study section. The results obtained are summarized in Table 2.

Table 2: Rock mass characterization in the study section

Sec	RQD	Jn	Jr	Ja	Jw	SRF	Q - value
A	70	4	3	2	1	1	26.25
B	60	4	3	2	1	1	22.5

For the GSI value, the chart included in [1] was used to evaluate the GSI. This value was further evaluated using the equation proposed by [1] using the Q-system's parameters:

$$GSI = \frac{52\,(J_r/J_a)}{1+J_r/J_a} + \frac{RQD}{2} \quad (3)$$

Table 3 contains the values of GSI calculated using Q-system parameters of respected sections.

Table 3: Calculation of GSI using Q parameters.

Section	RQD	Jr	Ja	Jr/Ja	GSI
A	70	3	2	1.5	66
B	60	3	2	1.5	61

Residual GSI value The intact rock properties are not reduced when the rock is fractured so the mechanical parameters σ_{ci} and m_i are the same only the volume of the block and roughness conditions of joints are altered. According to [5], the residual Hoek Brown constants for the rock mass may be calculated from a residual GSI_r value using the same formulae as for peak strength parameters. Thus, a GSI_r value of 20 was used for the residual condition in order to simulate a strain softening model.

Hoek-Brown parameters Hoek-Brown constant m_b for the rock mass, and s and a are constants which depend upon the rock mass characteristics. The material constants m_b, s and a were calculated using the following equations. The value for m_i for gneiss was taken as 23.

$$m_b = m_i\, exp\left(\frac{GSI-100}{28-14D}\right) \quad (4)$$

$$s = exp\left(\frac{GSI-100}{9-3D}\right) \quad (5)$$

$$a = \frac{1}{2} + \frac{1}{6}\left(e^{\frac{GSI}{15}} - e^{-\frac{20}{3}}\right) \quad (6)$$

Where D is the factor that depends upon the degree of disturbance due to blast damage and stress relaxation

[1]. The value of disturbance factor(D) is taken as 0.5 on the basis of the chart proposed by [1] as it was observed that the gneiss found in the cavern was of good quality and had moderate effects on surroundings; GSI of 65 was found appropriate based on the GSI characterization chart and correlation with Q-value parameters which was used for the calculation as a representative value of the whole section. The values of Hoek and Brown parameters obtained are:

Table 4: Hoek and Brown parameters for study section.

Item	Undisturbed zone Elastic	Res.	Disturbed zone Elastic	Res.
GSI	65	20	65	20
m_b	6.59	1.32	4.34	0.51
s	0.02047	0.00014	0.00940	0.00002
a	0.5022	0.5439	0.5022	0.5439

3.3 Evaluation of Rock Stresses

In-situ stresses in rock mass are the result of overlying strata, plate tectonics, and stresses due to topographic effects. Generally, in-situ stress is measured using methods like hydraulic fracturing, and 3D over coring. Since we don't have measured data for the selected site. So, we investigate reviewing similar nature projects. It was concluded by [6] that tectonic stress magnitude of 15 MPa with orientation N350°E is acting at the Upper Tamakoshi Hydropower project. From Figure 5 it can be approximated that trend of tectonic stress for Himalaya is NE-SW at the north-western part and around N-S towards the southeastern part. The project location has a similar orientation to that of UTKHP so we are using a similar value for tectonic stress. Still to confirm three-dimensional stress measurement is required and is proposed as a suggestion. To assess the stress situation, total stress can be measured directly using a stress cell or calculated using topography, overburden, and knowledge of the region's general stress conditions [8].

Due to the gravity of earth, there are two components of the gravitational stresses i.e. horizontal and vertical components. When the surface is horizontal, the vertical gravitational stress at a depth of h is:

$$\sigma_v = \gamma h \tag{7}$$

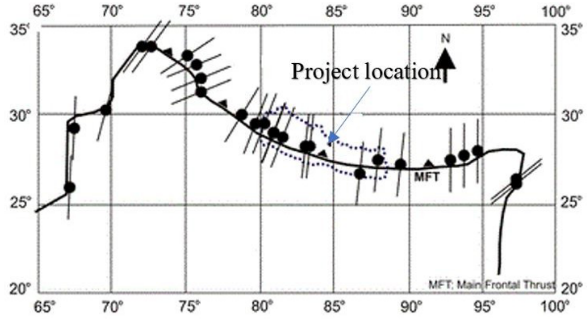

Figure 5: Approximate horizontal tectonic stress orientation [7].

In an elastic rock mass with a Poisson's ration of ν, the horizontal stress induced by gravity is:

$$\sigma_h = \frac{\nu}{1-\nu}\gamma h \tag{8}$$

According to [7], the magnitude of total horizontal stress can be calculated by:

$$\sigma_H = \frac{\nu}{1-\nu}\gamma h + \sigma_{tec} \tag{9}$$

Where, σ_v and σ_h are the vertical and horizontal stresses in MPa, σ_{tec} is the tectonic stresses (locked-in stress) due to plate tectonic movement, γ is the specific weight of rock mass in MN/m^3, and H is overburden depth in meters.

Since $Phase^2$ is a two-dimensional program, the horizontal stresses must be projected into the relevant cross-section for the model. This can be done from equation 10 and 11 derived from an equilibrium state in a two-dimensional stress plane [9].

$$\sigma_\alpha = \sigma_H cos^2\alpha + \sigma_h sin^2\alpha \tag{10}$$

$$\sigma'_\alpha = \sigma_H sin^2\alpha + \sigma_h cos^2\alpha \tag{11}$$

Where, σ_α and σ'_α ar in-plane and out-plane horizontal stresses and α is the angle between tunnel axis and minimum horizontal stress. The value of stress calculated for the numerical model is given in the Table 5.

4. Numerical Model for Powerhouse Cavern

A two-dimensional FEM program, $Phase^2$ [11], has been used to model and analyse the stability of the underground powerhouse cavern. The following simplifications and assumptions have been made:

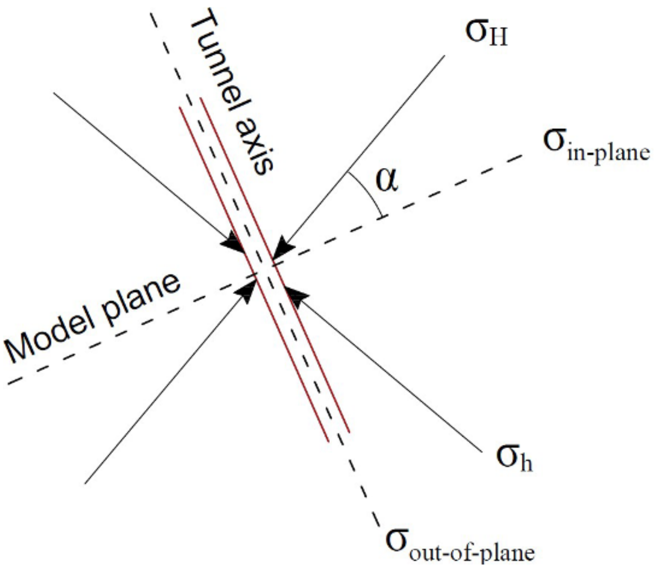

Figure 6: Illustration of the use of equation 10 and 11. [10]

- The surrounding rock mass is assumed to be homogeneous and continuous; the joint effect is considered using the equivalent deformation module, E.
- The initial in situ stress is uniformly distributed within the computational domain.
- It is assumed that the rock mass obeys the Hoek–Brown failure criterion.

4.1 Valley model

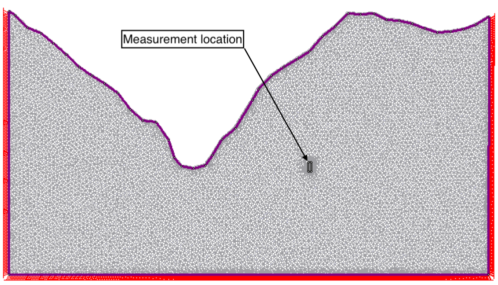

Figure 7: Topographical model of cross section and stress measurement location

The analysis problem is solved with a 2D topographical model. One cross-section, perpendicular to the length axis of the powerhouse cavern is used. The topographical profiles are imported from the working drawings of the hydropower project, and the topographical model of the cross-section is shown in Figure 7. The bottom boundary of the model is restrained in both X and Y directions, the sides are restrained in the X direction

Table 5: In-Situ Stress calculation

Input Parameters		
Overburden	335	m
Poissons Ratio	0.31	
Tectonic Stress	7.5	MPa
Trend of Tectonic Stress	N 350° E	
Cavern Trend	N 45°E	
Angle	35°	
Density of Rock	27	kN/m3
Stress due to Gravity		
Vertical Stress	9.045	MPa
Horizontal Stress	4.06	MPa
Total Horizontal Stress	11.56	MPa
In- Plane	9.09	MPa
Out of Plane	6.53	MPa
Locked in Stress		
In- Plane	5.03	MPa
Out of Plane	2.47	MPa

only, while the top surface is free to move in both directions. Further gravity-type field stress chosen, with the use of actual ground surface since the model profile has variable elevation. In order to study the stresses in the rock mass, the material is assumed to be elastic. In this way, the stresses can develop without any failure occurring in the material. In the laboratory, the unit weight of the banded gneiss is found to be 27 kN/m^3. Modelling is carried out as plane strain analysis using Gaussian eliminator as solver type. Both in-situ stress ratio (both in and out of plane) and locked-in horizontal stress for both in and out of plane used in the model have been summarized in Table 5.

Results of Valley Model The model was run with the loading conditions, as explained in the above sections with the aim to achieve the principal stresses at the location of the powerhouse cavern. The result from one of these simulations is shown in Figure 8. Table 6shows the results from the valley model, which contains maximum and minimum horizontal stress directions, and the obtained stresses at the point of the underground powerhouse cavern.

4.2 Model of Powerhouse Cavern

Model Setup A vertical cross-section of the cavern with its excavation stages was modelled. The

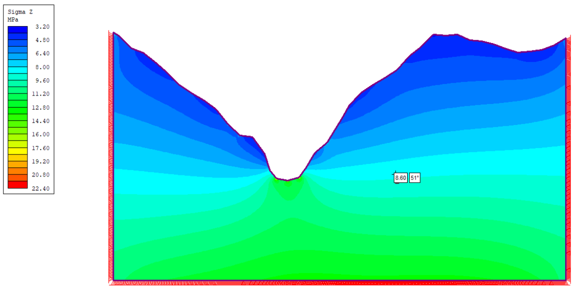

Figure 8: Simulation of stress conditions in the valley model (σ_1).

Table 6: Result of stress analysis

σ_1 (MPa)	σ_2 (MPa)	σ_3 (MPa)	σ_1 angle from horizontal (°)
10.3	5.18	8.6	51

excavation stages can be seen in the Figure 9. In order to ensure that the boundary is far away to simulate infinite conditions so that it doesn't influence the simulation an expansion factor of 5 with the "Box Boundary Type" option was used. The "Increase Mesh Element Density" option has been used to increase the element density around caverns in order to improve the results. All the nodes on the boundary were given fixed boundary condition with zero displacement. Figure 10 shows a cavern of 28m×14.5m

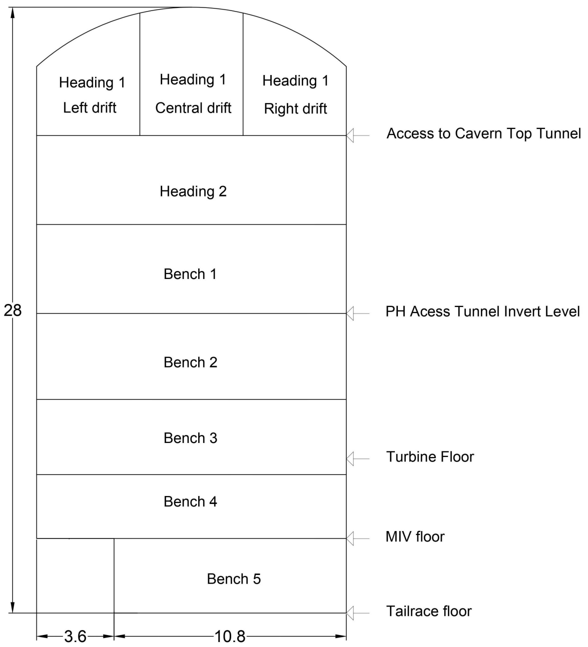

Figure 9: Excavation stages of Powerhouse Cavern.

cross-section modelled in *Phase*^{2} as described above. The obtained stress from stress analysis in Table 6 was used in this model. Since the primary purpose of this model is to design a thin (typically 0.2 m) shotcrete lining in a relatively large cavern, it is necessary to choose a mesh that will allow vertices to be spaced at approximately half the thickness of the shotcrete lining [12]. Widely spaced vertices in the beam elements used to model the shotcrete lining will have poorly distributed forces [12]. According to [12], a six-noded triangular element mesh gives good results and the vertex spacing on the excavation border must be precisely defined. Hence, the six-noded element mesh option was chosen and the vertex on the excavation boundary was set 100mm apart. A disturbance zone of radius 2m having decreased strength was also included in the model.

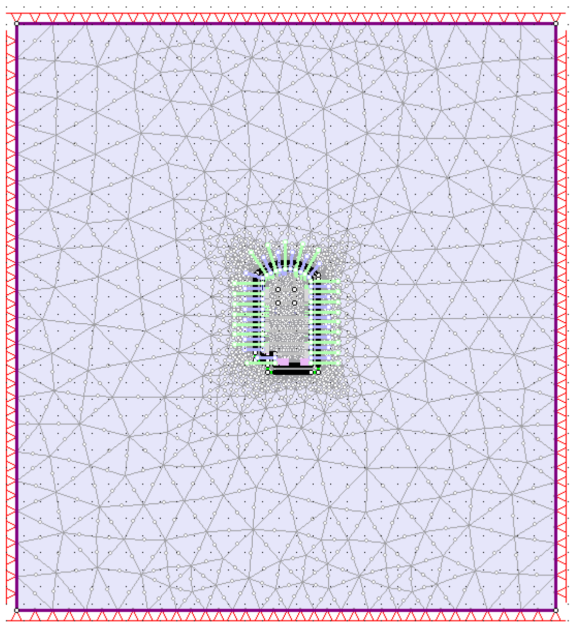

Figure 10: Model of powerhouse cavern profile and excavation stages in *Phase*^{2}.

Rock support considerations Rock support should be planned so that a stable condition is attained during every stage of excavation as well as the last stage. Several factors, including excavation stages, rock mass behaviour, and construction restrictions, should be taken into account to achieve the best rock support measure. There are numerous excavation stages in the powerhouse cavern, and in general, a larger excavation results in more adverse stress redistribution, more displacement, and possibly more support. Rock support required in the early stages may be heavier than necessary to support heavier loads from later stages of excavation. It can be assumed that support for the later stages could be installed as soon as possible in this regard which isn't the case. Rock mass behaves such that the need for rock support capacity will be drastically reduced if a certain relaxation of rock mass around an opening is permitted. It is economic to permit some delay in the support installation. The delay must occur during a stand-up period during which stability is still maintained. The rock support for the powerhouse cavern needs to be planned so that the excavation phases are followed. For the rock mass to relax, a certain amount of time must pass, and it must also match the capacity of the construction equipment. The numerical modelling should take into account each of these concerns. FEM program *Phase*^{2} is used to model the rock excavation and the support. A combination of fully cement grouted rock bolts and shotcrete has been used in the model for rock support. Rock bolts are installed in weak rock masses to keep rocks in a place where stresses have exceeded strength. This failed rock still possesses a reduced but finite strength which can produce confining stresses that help to stabilize the surrounding rock mass. The short rock bolts are designed to create a bolt-rock ”shield” around the opening, while the long bolts are used to suspend the shield to strong rock formations behind the failure zone [13]. Shotcrete is modelled using a ”composite element” to account for the time effect on rock mass relaxation and the stage of application of various layers of shotcrete. With this element,shotcrete has several layers (assumed to be 10 cm each) and can be applied at different delaying times. After trying many options, the adopted support procedure for detailed analyses is given in the Table 7.

Table 7: Rock support and excavation procedure

Stage	Exc.	Stress	Rock Bolt		Shotcrete	
		Relax	5m	8m	1st	2nd
1	No Excavation					
2	1(1)	50%				
3		50%	1(1)		1(1)	
4		100%				
5	1(2)	50%				
6		50%	1(2)		1(2)	
7		100%				
8	2	50%				
9		50%	2		2	
10		100%				
11		100%		1,2		1,2
12	3	50%				
13		50%	3		3	
14		100%				
15	4	50%				
16		50%	4		4	
17		100%				
18		100%		3,4		3,4
19	5	50%				
20		50%	5		5	
21		100%				
22	6	50%				
23		50%	6		6	
24		100%				
25		100%		5,6		5,6
26	7	50%				
27		50%	7		7	
28		100%				
29		100%		7		7

Modelling and results Numerical modelling follows up on the recommended excavation and support steps in Table 7. Ground relaxation was modelled by applying a uniformly distributed load to the excavation profile at each stage of excavation in the numerical model. 50% ground relaxation was allowed in the analysis before the installation of the support system. Understanding the stages of excavation, the behaviour of rock mass displacement, and the interaction of the support measures are crucial for achieving a reasonable design of a support system. According to the analyses, early bolt application would create a stable foundation and stop rock blocks from becoming loose. Due to the displacement characteristic of the rock mass, applying a single, thick shotcrete layer at a very early stage is not advised. The displacement of the rock mass changes according to the depth of the excavation and the amount of time needed for stress redistribution. As a result, it is best to install the shotcrete in multiple layers and to time it to match the construction schedule provided by the numerical modelling.

The Figure 11 shows the displacement observed in the powerhouse cavern with the applied support. The roof is able to remain largely stable thanks to the bolt system and first layer of shotcrete. However, there are a few minuscule locations where the model's line elements show signs of yielding by colouring them red. As a result, both in reality and in the model, the second layer of shotcrete must be applied before the next benching. In the final stage, when the final benching and supporting work is completed, the support for the cavern is system bolting of 5 m long, 3

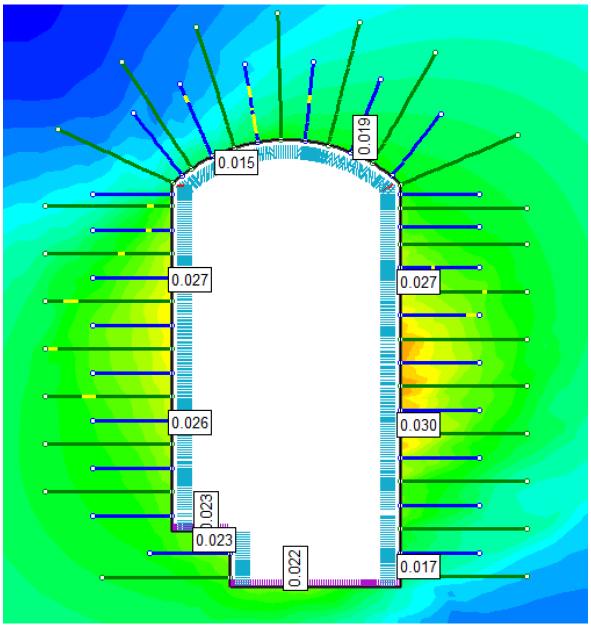

Figure 11: Total displacement and yielded elements at the final stage.

m spacing and 8 m long, 3 m spacing with 2 layers of shotcrete of thickness 100 mm each. A maximum displacement of 30mm in the walls was observed in the model.

5. Conclusion

The design for excavation and support for the powerhouse cavern should include all of the geotechnical characteristics and topographical features. The numerical model was established to include the mentioned geological properties. The in-situ stress field used in the model was the stresses calculated from topographical, gravitational and tectonic effects. Rock mass deformation in relation to the excavation stages was also investigated. The support measures, such as systematic bolting and layer-by-layer shotcrete, were implemented in the recommended order. This also complied with the building processes to produce a technically sound and cost-effective design. The model demonstrated that the proposed support measures make the cavern stable. On the right wall, the maximum displacement result from the model was about 30 mm. The analyses show that a close integration between real-world experience and numerical modelling is necessary for the design of excavation and supporting work.

Acknowledgments

The authors would like to express their thanks to Peoples Hydropower Company for permission to prepare and publish this paper.

References

[1] Evert Hoek. *Practical Rock Engineering*. www.rocscience.com, 2007.

[2] Chhatra Bahadur Basnet and Krishna Kanta Panthi. Detailed engineering geological assessment of a shotcrete lined pressure tunnel in the himalayan rock mass conditions: a case study from nepal. *Bulletin of Engineering Geology and the Environment*, 79:153–184, 1 2020.

[3] Krishna Kanta Panthi. Review on the prevailing methods for the prediction of potential rock burst / rock spalling in tunnels. 2017.

[4] E. Hoek and M.S. Diederichs. Empirical estimation of rock mass modulus. *International Journal of Rock Mechanics and Mining Sciences*, 43(2):203–215, 2006.

[5] M. Cai and P. Kaiser. In-situ rock spalling strength near excavation boundaries. *Rock Mechanics and Rock Engineering*, 47, 02 2014.

[6] Chhatra Basnet and Krishna Panthi. 3d in-situ stress model of upper tamakoshi hydroelectric project area. 21:34.

[7] Krishna Kanta Panthi. Effectiveness of post-injection grouting in controlling leakage: A case study. *Hydro Nepal: Journal of Water, Energy and Environment*, 8:14–18, 10 2012.

[8] Bjorn Nilsen and Arild Palmström. *Engineering Geology and Rock Engineering : Handbook. No. 2*. Norwegian Group for Rock Mechanics, Oslo, 2000.

[9] Charlie C. Li. *Applied Rock Mechanics*. Norwegian University of Science and Technology, 2015.

[10] Ragna Torås Halseth. Stability assesment of the headrace tunnel system at brattset hydropower project. 2018.

[11] Rocscience Inc. Rocscience RS2 User Guide, 2022. [Online; accessed 2022-08-16].

[12] Evert. Hoek. Cavern reinforcement and lining design. 2011.

[13] Charlie Li. Principles of rockbolting design. *Journal of Rock Mechanics and Geotechnical Engineering*, 9, 05 2017.